The Agulhas Plateau: structure and evolution of a Large Igneous Province

N. Parsiegla, K. Gohl and G. Uenzelmann-Neben

Alfred Wegener Institute for Polar and Marine Research, PO Box 12161, 27515 *Bremerhaven, Germany. E-mail: Nicole.Parsiegla@awi.de*

SUMMARY

Large Igneous Provinces (LIP) are of great interest due to their role in crustal generation, magmatic processes and environmental impact. The Agulhas Plateau in the southwest Indian Ocean off South Africa has played a controversial role in this discussion due to unclear evidence for its continental or oceanic crustal affinity. With new geophysical data from seismic refraction and reflection profiling, we are able to present improved evidence for its crustal structure and composition. The velocity–depth model reveals a mean crustal thickness of 20 km with a maximum of 24 km, where three major units can be identified in the crust. In our seismic reflection records, evidence for volcanic flows on the Agulhas Plateau can be observed. The middle crust is thickened by magmatic intrusions. The up to 10 km thick lower crustal body is characterized by high seismic velocities of 7.0–7.6 km s^{-1}. The velocity–depth distribution suggests that the plateau consists of overthickened oceanic crust similar to other oceanic LIPs such as the Ontong-Java Plateau or the northern Kerguelen Plateau. The total volume of the Agulhas Plateau was estimated to be 4×10^6 km^3 of which about 10 per cent consists of extruded igneous material. We use this information to obtain a first estimate on carbon dioxide and sulphur dioxide emission caused by degassing from this material. The Agulhas Plateau was formed as part of a larger LIP consisting of the Agulhas Plateau itself, Northeast Georgia Rise and Maud Rise. The formation time of this LIP can be estimated between 100 and 94 ($\pm$ 5) Ma.

Key words: Controlled source seismology; Oceanic plateaus and microcontinents; Large igneous provinces; Crustal structure; Volcanic gases; Africa.

1 INTRODUCTION

Large Igneous Provinces (LIP) are voluminous emplacements of extrusive and intrusive rocks (e.g. Coffin & Eldholm 1994). Continental flood basalts, oceanic basin flood basalts, oceanic plateaus, volcanic rifted margins, and aseismic ridges make up the various types of LIPs (e.g. Coffin *et al.* 2006). Causes and consequences of LIP formation are still poorly understood and include a great variety of aspects including geodynamic, thermodynamic, geochemical and petrologic issues. Of particular interest are interactions between LIP emplacement and continental breakup and rifting, discussions about their sources, and LIPs as a mechanism for heat release. LIPs provide a possibility to investigate petrologic and geochemical properties of the mantle. Growing interest has been attracted to climate and environmental consequences of LIP formation during the last years (e.g. Saunders 2005; Wignall 2005).

The Agulhas Plateau is an oceanic plateau south of South Africa in the SW Indian Ocean (Fig. 1). Scrutton (1973) suggested a composition of oceanic crust from an abandoned spreading centre. Other authors identify the northern Agulhas Plateau with its rough topography to consist of thickened oceanic crust (Barrett 1977) whereas the southern plateau is argued to be composed of continental fragments (Tucholke *et al.* 1981; Angevine & Turcotte 1983). Studies by

Uenzelmann-Neben *et al.* (1999) and Gohl & Uenzelmann-Neben (2001) were based on seismic reflection and refraction data on the southern Agulhas Plateau and identify the plateau as an oceanic LIP. They derived a crustal thickness of 25 km with high seismic velocities of 7.0–7.6 km s^{-1} for the lower part of the crust.

Those controversial results on the oceanic or continental origin of this plateau justified the collection of additional geophysical data across the plateau's central and northern part. Improved evidence for either continental or oceanic affinity would have consequences for the role the plateau played in the regional supercontinental assembly and breakup. If the plateau consists of continental fragments, their origin and correlation to conjugate continental platforms have to be investigated in order to solve their fit into the jigsaw of plate-kinematic reconstructions. If the plateau is an oceanic LIP, questions regarding the time of its formation and consequences of the excessive magmatic emplacement have to be addressed.

2 GEOLOGICAL AND TECTONIC BACKGROUND

The Agulhas Plateau is located in the present southwestern Indian Ocean where the Gondwana breakup between Africa, South
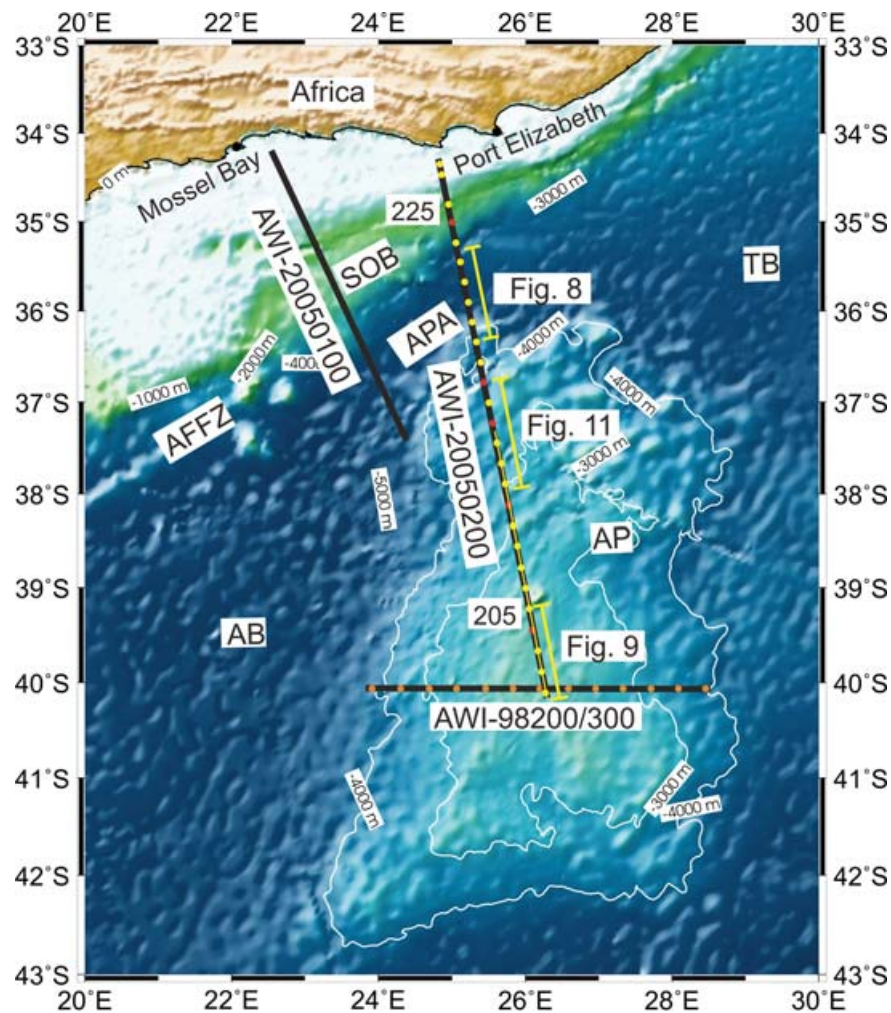
336

Figure 1. Overview map of the area of investigation with satellite derived topography (Smith and Sandwell, 1997) and location of seismic refraction lines AWI-98200/300 (orange), and AWI-20050200 (yellow) used in this paper (Figs 6 and 10). Dots represent positions of ocean bottom seismometers (OBS), red dots mark OBS positions where data are shown in Figs 3 and 4, thick black lines correspond to the shot profiles, yellow bars mark coincident seismic reflection sections AWI-20050201 (Figs 8, 9 and 11), the thin yellow line through the southern OBS stations of profile AWI-20050200 shows the position of the coincident shipborne magnetic profile (Fig. 6). Positions of OBS stations 205 and 225 are labelled. Abbreviations are AB, Agulhas Basin; AFFZ, Agulhas-Falkland Fracture Zone; AP, Agulhas Plateau; APA, Agulhas Passage; SOB, Southern Outeniqua Basin and TB, Transkei Basin.

America and Antarctica occurred in the Cretaceous. Today, the plateau rises up to 2500 m above the surrounding seafloor and covers an area of more than 230 000 km². It therefore presents a major bathymetric high in this region which is limited to the north by the 4700 m deep Agulhas Passage and is flanked by the Agulhas Basin in the west and the Transkei Basin in the northeast. The northern part of the plateau exhibits a rugged topography and basement morphology (Allen & Tucholke 1981), while the central and southern part of the plateau is characterized by mostly smooth topography and basement (Allen & Tucholke 1981).

The African, South American and Antarctic plates are joined at the Bouvet triple junction (54.5°S and 1°W). Plate-tectonic reconstructions show that this triple junction was situated near the southwestern tip of the Agulhas Plateau at about 96 Ma (Marks & Tikku 2001). Marks & Tikku (2001) interpret the topographic high, which extends from the southwestern Mozambique Ridge to the southern Agulhas Plateau (Fig. 2), as the path of the Bouvet triple junction. According to Hartnady & le Roex (1985) and Martin (1987), the Bouvet hotspot track crossed the northern part of the Agulhas Plateau at approximately 100 Ma (Fig. 2) and was

therefore thought to have controlled the formation of the Agulhas Plateau together with nearby spreading centres between 80 and 100 Ma (Uenzelmann-Neben *et al.* 1999; Gohl & Uenzelmann-Neben 2001). Kristoffersen & LaBrecque (1991) and Gohl & Uenzelmann-Neben (2001) suggest a joint formation of the Agulhas Plateau together with Northeast Georgia Rise and Maud Rise. This combined area of 0.5×10^6 km² makes the size comparable to that of the Broken Ridge LIP or a third of the Kerguelen Plateau.

3 DATA ACQUISITION AND PROCESSING

The Alfred Wegener Institute for Polar and Marine Research (AWI) acquired marine seismic reflection and refraction/wide-angle reflection data (Uenzelmann-Neben 2005) along two profiles across the southern continental margin of South Africa and the Agulhas Plateau (Fig. 1) during the R/V Sonne cruise SO-182 as part of the Agulhas-Karoo Geoscience Transect in the German–South African cooperative project Inkaba ye Africa (de Wit & Horsfield 2006). Details of the western profile (Fig. 1, AWI-20050100) are described
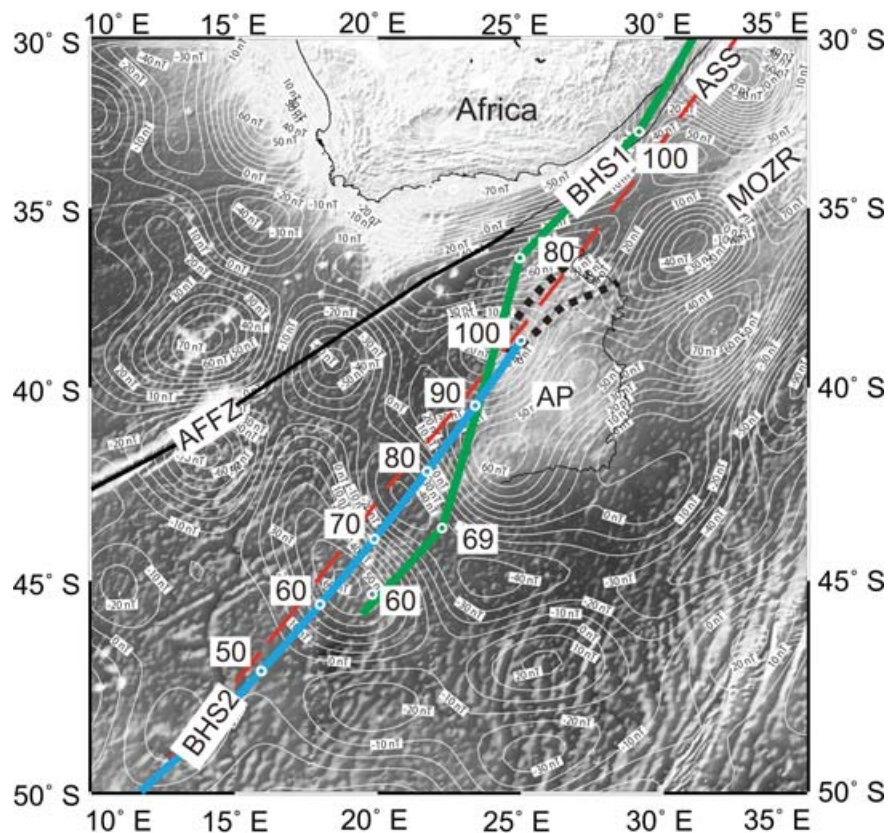
Figure 2. CHAMP magnetic anomalies (Maus *et al.* 2007) drawn as white isolines with 10 nT contour interval overlying the satellite derived topography (Smith & Sandwell 1997). Hotspot paths are drawn with thick lines and white circles with annotated times of the hotspot passage. Black dotted lines indicate graben-like lineations in the northern Agulhas Plateau. The southern boundary of the African Superswell (Nyblade & Robinson 1994) is marked with a red dashed line. Abbreviations are AFFZ, Agulhas-Falkland Fracture Zone; AP, Agulhas Plateau; ASS, southern boundary of the African Superswell; BHS1, Bouvet hotspot path after Martin (1987); BHS2, Bouvet hotspot path after Hartnady & le Roex (1985) and MOZR, Mozambique Ridge.

in Parsiegla *et al.* (2007). The 670 km long eastern profile AWI-20050200 (Fig. 1) stretches from the Outeniqua Basin to the southern Agulhas Plateau, crossing the Agulhas Passage and the Agulhas-Falkland Fracture Zone. We deployed 27 ocean-bottom seismometers (OBS) with an average spacing of 20 km. Airgun shots from eight G.Guns™ and one large-volume Bolt airgun with a total volume of 96 l were discharged every 60 s, corresponding to a nominal shot spacing of 150 m. The OBS data were corrected for clock drift and relocated using the water wave arrival. A bandpass filter of 4–17 Hz and an automatic gain control with a 0.5 s window were applied before traveltime picking of refracted and wide-angle reflected phases. Most of the OBS records produced good to very good quality *P*-wave arrivals with maximum offsets up to 250 km in the vertical components (e.g. Figs 3 and 4), while *S*-wave data are of considerably lower quality and therefore could not be used for crustal analysis.

Normal-incidence seismic reflection data were recorded simultaneously with a sampling rate of 2 ms using a 180-channel streamer (2250 m active length, SERCEL SEAL™ system). These data were processed in a standard processing flow to depth-migrated sections. The processing flow comprised sorting (50 m CDP interval), a detailed velocity analysis to invoke the subsurface topography (every 50 CDPs), multiple suppression via a Radon transform filtering method, corrections for spherical divergence and normal moveout, application of streamer corrections, stacking, and migration. An Omega-X migration was carried out both in time and depth domain (Yilmaz 2001). This method allows vertical variations in

velocity and is accurate for large dips ($\leq 85°$, Yilmaz 2001). The stacking velocities, which were converted into interval velocities using Dix's formula, were used to set up the velocity field used for the migration process and the embedded conversion from time to depth. The onboard SIMRAD and Parasound systems of RV Sonne recorded continuous multibeam bathymetry and subbottom profiler data. In addition, we use pre-existing crustal seismic refraction data of profiles AWI-98200 and AWI-98300 across the Agulhas Plateau (Fig. 1) (Uenzelmann-Neben *et al.* 1999; Gohl & Uenzelmann-Neben 2001).

During the return track of RV *Polarstern* cruise ANT-XXIII/4 in 2007, shipborne magnetic data were collected along the southern 300 km of profile AWI-20050200 (between 360 and 660 km of profile distance, Fig. 1).

4 MODELLING

4.1 Seismic traveltime inversion

We identified *P*-wave traveltimes for profile AWI-20050200, where 24 stations yielded useful *P*-wave data. Pick uncertainties were set in the range from 40 to 150 ms, depending on the signal-to-noise ratio. We modelled the velocity–depth distribution using the 2-D traveltime inversion routine RAYINVR of Zelt & Smith (1992). Station locations and shots were projected onto a line fitted through the OBS positions.
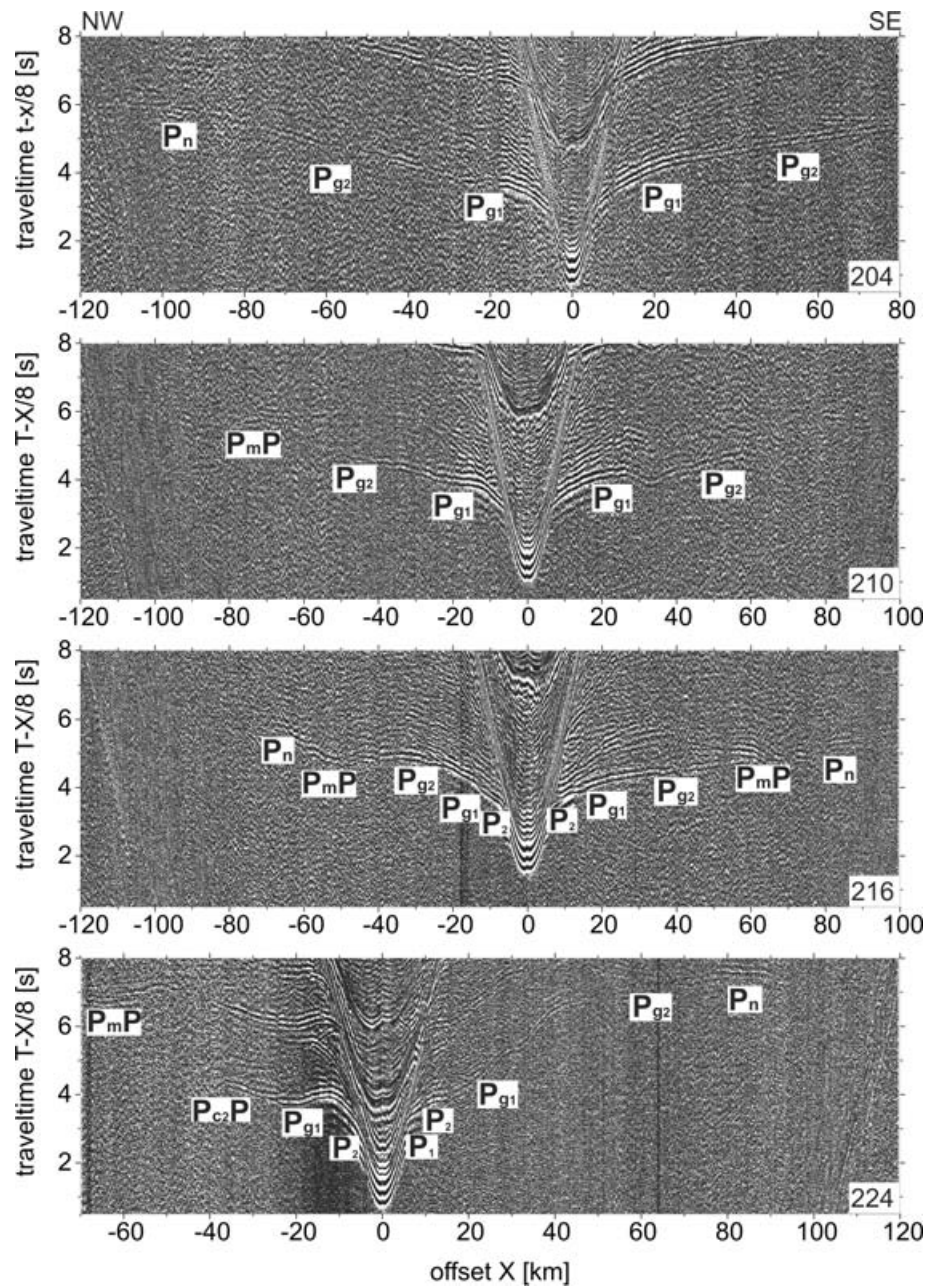
Figure 3. Seismic refraction data of the four OBS stations 204, 210, 216 and 224 along profile AWI-20050200 with annotated phases. For an explanation of the phases, see Table 1.

According to the main groups of identified traveltime branches from the OBS records (Table 1), we parametrized our initial model into five model layers beneath the water-layer with the crust (including sediments) represented by layers 1–4, and the upper mantle represented by layer 5. The horizontal spacing of the velocity nodes was chosen with respect to OBS station distance and ray coverage. It lies between 33 and 45 km for layers 1–4.

The refracted arrivals from the uppermost crustal layer 1 are sparse because they are masked by the arrival of the direct water-wave. Thus, the lower boundary of this layer was aligned with our interpretation of the acoustic basement from the near-vertical seismic reflection recordings. This basement was clearly identified for model distances 118–210, 279–309, 379–411 and 550–652 km. For these model distances, the depth values were kept constant during

the inversion process. In the shelf area, this layer was difficult to identify in the near-vertical seismic reflection data. In other locations, layer 1 is very thin or the acoustic basement crops out.

A simple start model was improved by forward modelling. The resulting model of relatively good fit between observed and calculated traveltimes went into a traveltime inversion applied in a layer-stripping manner. The model quality was continuously assessed in the inversion process (Table 2). Fits between measured and modelled traveltimes are summarized in Fig. 5. The calculated traveltimes for the final model (Fig. 6a) have an overall rms deviation from the observed traveltimes of 0.128 s and a χ^2-value of 1.3, which is close to the optimum value of 1. The resolution kernels are calculated for the velocity (Fig. 7a) and depth nodes (Fig. 7b) of the final model. Nodes with a resolution greater than 0.5 (range is 0–1) are
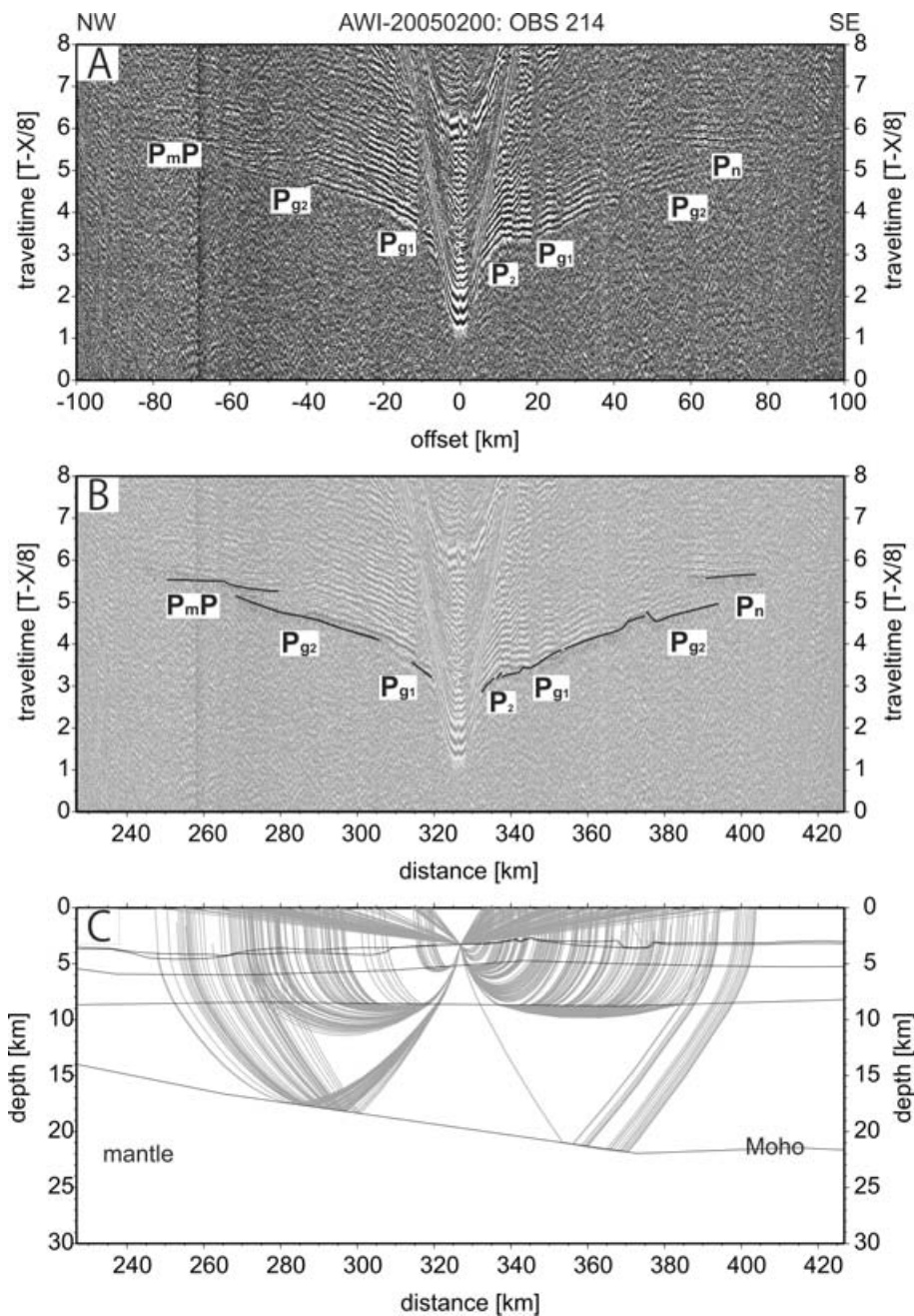
Figure 4. Seismic refraction data of OBS station 214 along profile AWI-20050200. The seismogram with annotated phases (a), picks and modelled traveltime curves (b) and ray paths (c) are shown. For an explanation of the phases, see Table 1.

considered as well resolved (Zelt & White 1995). For all layers more than 70 per cent of the depth nodes are well resolved (Fig. 7b). Less resolved depth nodes are mainly located in regions with low ray coverage at the beginning and the end of the profile (Fig. 7c). The velocity nodes of the first layer are reasonably resolved until 100 km model distance (Fig. 7a). The velocity resolution decreases farther south, although most of the layer thickness is constrained by our multichannel reflection data. The second layer is well resolved with only small regions at its lower zone having a resolution of less than 0.5 (Fig. 7a). As more rays penetrate and turn at the top of the layers (due to their incidence angle and the velocity gradient in the layer), the lower layer zones are usually less resolved. The third and fourth layers are well resolved for most parts. The fourth layer is well re-

solved at the Agulhas Plateau but poorly resolved in the northern part of the profile because of a low ray coverage (Fig. 7c). As the resolution depends on the number of velocity–depth nodes as well as on the number of rays, the ray coverage provides a qualitative illustration of the model accuracy (Fig. 7c). Layer 3 is very well covered by rays which constrain velocities from the top to the bottom of this layer. As the resolution and the ray plot (Fig. 7) show, the velocity–depth model (Fig. 6a) is only moderately constrained in the lower crust (layer 4) for the first 130 km profile distance. Farther south, the model is much better constrained. Rays of refracted waves mainly turn in the upper third of this layer, except for two regions (130–200 km and 460–580 km profile distance) where rays cover almost the whole thickness of the layer. The crust–mantle boundary (Moho)

Table 1. Phase names of *P*-waves identified in the seismic refraction data and their explanation. The last column states the number of stations where a certain phase could be identified.

Name	Type	Origin	Stations
P_1	Refracted *P*-wave	Model layer 1	3
Ps_1P	Reflected *P*-wave	Top of model layer 2	3
P_2	Refracted *P*-wave	Model layer 2	13
Pc_1P	Reflected *P*-wave	Top of model layer 3	5
Pg_1	Refracted *P*-wave	Model layer 3	24
Pc_2P	Reflected *P*-wave	Top of model layer 4	7
Pg_2	Refracted *P*-wave	Model layer 4	20
PmP	Reflected *P*-wave	Top of model layer 5	14
Pn	Refracted *P*-wave	Model layer 5	12

Table 2. Statistics of *P*-wave traveltime inversion. Number of traveltime picks, the root-mean squared (rms) error of the fitting, and the χ^2 value of the different phases.

Phase name	Picks	rms	χ^2
P_1	56	0.076	1.073
Ps_1P	29	0.048	0.260
P_2	296	0.115	1.921
Pc_1P	66	0.081	0.545
Pg_1	2071	0.114	1.309
Pc_2P	131	0.076	0.464
Pg_2	2829	0.133	1.328
PmP	701	0.140	1.285
Pn	824	0.149	1.290

is constrained by large-amplitude wide-angle reflections (PmP) and upper mantle refraction (Pn) phases. They define the Moho depth and add information on the velocity–depth structure of the lower crust. The upper mantle is sampled by rays reaching up to 4 km beneath the Moho.

4.2 Modelling results

In the final *P*-wave velocity–depth model (Fig. 6a), layer 1 consists of sediments with velocities between 1.7 and 3.4 km s^{-1}. From 0 to 90 km profile distance, this layer is up to 1.7 km thick. The sedimentary basins of the South African shelf are located in this region. In the Agulhas Passage the sediments are up to 1.3 km thick (Fig. 8). Only small patches of sediments of some 100 m thickness exist on the northern Agulhas Plateau. From 550 to 650 km inline distance (CDP 11 000–13 000), sediments reach up to 0.7 km thickness (Fig. 9). Layer 2 has velocities between 3.4 and 4.5 km s^{-1} and a thickness between 0.6 and 1.1 km beneath the shelf region. Farther south this layer thickens to an average thickness of 1.2 km. Beneath the Agulhas Passage and the northern Agulhas Plateau velocities range between 3.3 and 5.3 km s^{-1}. Layer 2 velocities in the middle/southern Agulhas Plateau are between 3.3 and 4.7 km s^{-1}. Figs 8 and 9 show volcanic flows in layer 2. Layer 3 (Fig. 6a) exhibits velocities between 5.2 and 6.4 km s^{-1} in the shelf region, between 5.6 and 6.7 km s^{-1} beneath the Agulhas Passage, and 5.3–6.7 km s^{-1} in the Agulhas Plateau. In the northern part of the profile, this upper crustal layer has a maximum thickness of 12 km, and thins considerably down to 2 km in the Agulhas Passage. On the northern Agulhas Plateau layer 3 is 2.5–4.0 km thick and on the central to southern plateau 3.5–6.0 km. In model layer 4 velocities are between 6.5 and 6.6 km s^{-1} beneath the shelf, 6.8–7.2 km s^{-1} at the Agulhas Passage and range between 6.7 and

7.6 km s^{-1} in the lower crustal part of the Agulhas Plateau. Noteworthy is a well-resolved subvertical zone (centred at 370 km profile distance) of relatively low velocities of less than 7.0 km s^{-1} compared to lower crust north and south of it with velocities between 7.0 and 7.6 km (Fig. 6a). Above this zone, a northeast-trending trough of about 700 m depth can be observed in the ocean-floor. The Moho shows a kink here, changing its trend from southerly down dipping to almost horizontal. The Moho depth along the profile ranges from 31 km beneath the continental shelf and thins from 30 to 12 km in the Agulhas Passage. At the northern Agulhas Plateau, the Moho depth increases from 15 to 22 km followed by an almost constant depth of 23 km on average. The crustal thickness ranges from 30 km in the northern part of the profile, 8–14 km in the Agulhas Passage, 11–20 km at the northern part of the Agulhas Plateau, and 20 km in the central part on average. Upper mantle velocities range from 7.7 to 8.0 km s^{-1}. A comparison of our velocity–depth model (Fig. 6a) in the central and southern Agulhas Plateau region with the velocity–depth model of the combined profiles AWI-98200/98300 (Fig. 10) shows a similar velocity structure.

Most of the magnetic anomalies (Fig. 6b) along the southern part of the seismic profile are positive with a maximum amplitude of 1055 nT. Only three regions (367–375, 431–448 and 569–591 km profile distance) exhibit negative magnetic anomaly values. The lowest magnetic anomaly of −296 nT is found at 372 km profile distance, which coincides with the position of the subvertical zone of relatively low velocities in the velocity–depth model (Fig. 6a).

5 CRUSTAL TYPE AND STRUCTURE

The Agulhas Plateau has an average crustal thickness of 20 km which can be attributed to either thickened oceanic crust or extended continental crust. In layer 2, with average velocities of 4.1 km s^{-1}, layers of volcanic flows could be identified in our seismic reflection sections (Fig. 9). These are interpreted as a product of extrusive volcanism. Evidence for extrusive volcanism has previously been found on the southern part of the Agulhas Plateau (Uenzelmann-Neben *et al.* 1999; Gohl & Uenzelmann-Neben 2001) and could be identified as a continuous layer covering major parts of the plateau in this study (e.g. Figs 6a, 9, and 11). Basalt flows, which have also been dredged on the Agulhas Plateau (Allen & Tucholke 1981), make up major portions of this layer. Gladczenko *et al.* (1997) identify a similar layer with average velocities of 4.5 km s^{-1} on the Ontong Java Plateau. Upper to mid crustal velocities on the Agulhas Plateau of 5.3–6.7 km s^{-1} are comparable to average velocities of the middle crust of the Ontong Java Plateau (5.3 and 6.6 km s^{-1}) (Gladczenko *et al.* 1997). The average lower crustal velocity of the Agulhas Plateau of 7.2 km s^{-1} is slightly higher than that of the Ontong Java Plateau of 7.1 km s^{-1} (Gladczenko *et al.* 1997). On the Agulhas Plateau, the lower crustal body (LCB) with *P*-wave velocities between 7.0 and 7.6 km s^{-1} makes up about 50 per cent of the total crustal thickness (Fig. 6). These high seismic velocities are comparable to lower crustal velocities observed on the northern Kerguelen Plateau (Charvis *et al.* 1995) and the North Atlantic Volcanic margin (Eldholm & Grue 1994; Voss & Jokat 2007). The up to 10-km-thick high-velocity LCB of the Agulhas Plateau can be interpreted to consist of mafic to ultramafic material (Eldholm & Coffin 2000) and is a typical feature of oceanic plateaus (Eldholm & Coffin 2000; Coffin *et al.* 2006). The velocity–depth structure of the Agulhas Plateau is typical for overthickened oceanic crust observed at oceanic Large Igneous Provinces such as the Ontong Java Plateau (Gladczenko *et al.* 1997) and northern Kerguelen Plateau (Charvis
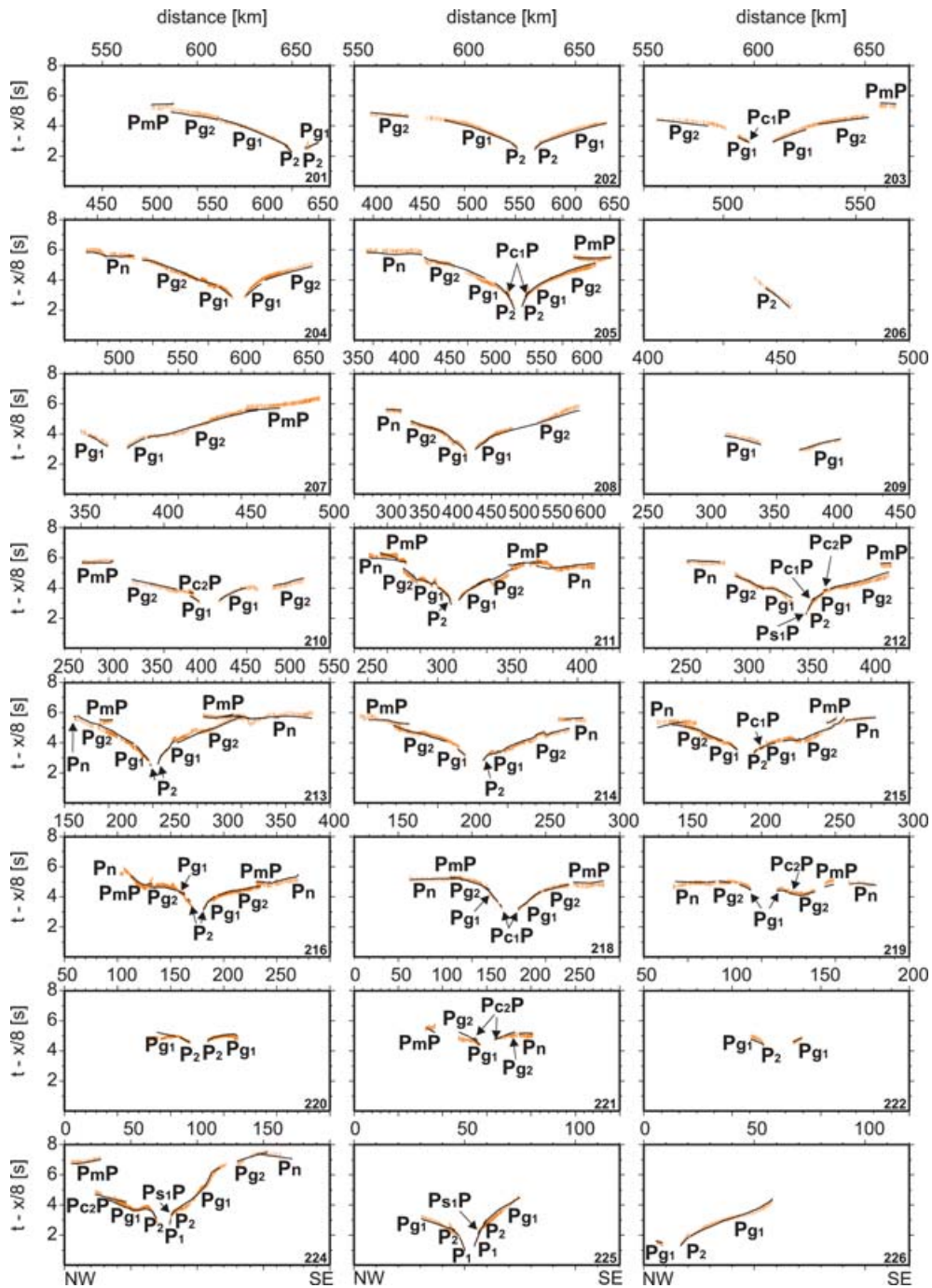
Figure 5. Picked (orange vertical bars) and modelled (black solid lines) seismic traveltimes. The length of the vertical error bars for the picked traveltimes corresponds to the assigned picking uncertainties. For an explanation of the phases, see Table 1.

et al. 1995). In comparison, average velocities as low as 6.7 km s^{-1} were observed in the lower crust of oceanic LIPs with large continental fragments such as the southern Kerguelen Plateau (Operto & Charvis 1996). We therefore conclude that the crust of the Agulhas Plateau must primarily be of oceanic affinity (Uenzelmann-Neben *et al.* 1999; Gohl & Uenzelmann-Neben 2001).

Allen & Tucholke (1981) and Tucholke *et al.* (1981) interpreted geochemical analyses of dredged rock samples as indications for continental fragments in the southern part of the Agulhas Plateau. If any continental fragments of felsic composition, and of sizes which are seismically resolvable, are included in the plateau crust,

zones of velocities lower than that of the mafic surroundings can be expected. Our velocity–depth model (Fig. 6) shows a distinct subvertical zone with velocities lower than those in the surrounding crust which coincides with a Moho kink at 370 km model distance. This zone coincides with a negative magnetic anomaly. A low-velocity anomaly within an oceanic plateau could be caused by embedded continental fragments. Previous geophysical studies have not confirmed any continental affinity (Uenzelmann-Neben *et al.* 1999; Gohl & Uenzelmann-Neben 2001). Although large-scale continental crust, as found on the southern Kerguelen Plateau, can be excluded for the Agulhas Plateau, it may still be possible
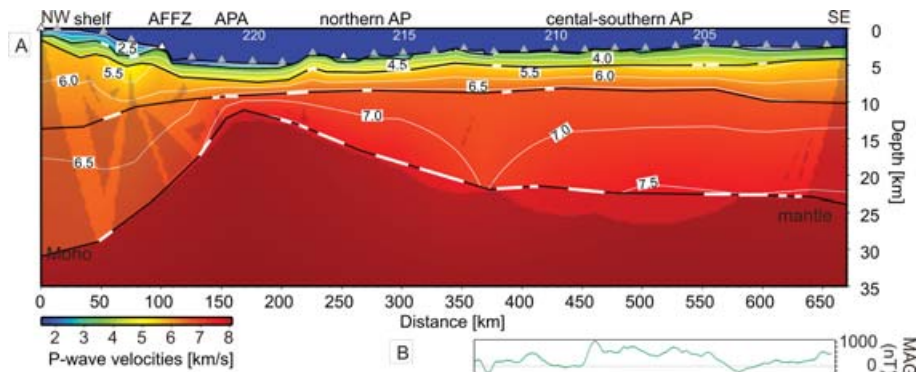
Figure 6. (a) Seismic *P*-wave velocity–depth model of profile AWI-20050200. Grey triangles mark OBS positions and numbers over triangles indicate station numbers. White triangles mark OBS which did not record any data. Black lines represent model layer boundaries with thick white lines marking positions of reflected phases at these boundaries. Thin white lines are velocity isolines. Dark shaded areas are not covered by rays. Abbreviations are AFFZ, Agulhas-Falkland Fracture Zone; AP, Agulhas Plateau; APA, Agulhas Passage. (b) Magnetic anomalies from shipborne measurements along this profile from 360 to 660 km profile distance.
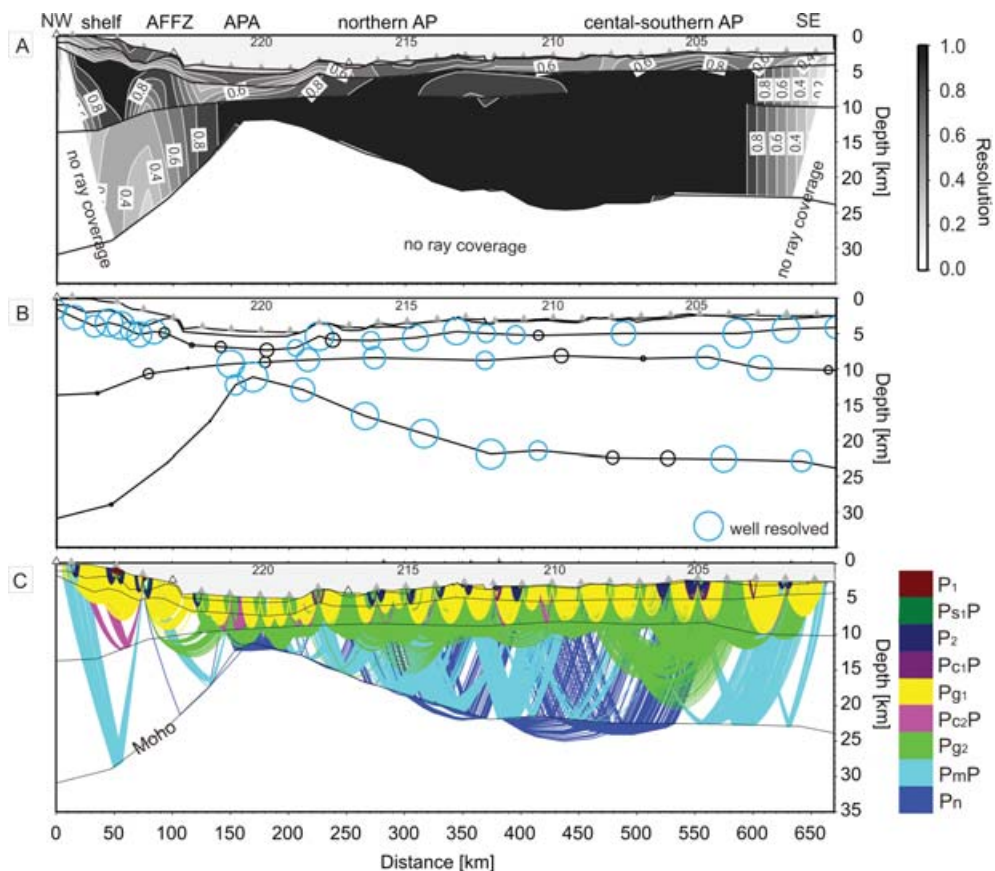

Figure 7. (a) Resolution of the velocity nodes of the velocity–depth model of profile AWI-20050200. Abbreviations are AFFZ, Agulhas-Falkland Fracture Zone; AP, Agulhas Plateau; APA, Agulhas Passage. Contour lines are drawn with an interval of 0.1. A value higher than 0.5 represents good resolution. Grey triangles are OBS positions, white triangles refer to stations which did not record any data and numbers over triangles indicate station numbers. (b) Resolution of depth nodes of the velocity–depth model. Blue circles represent a good resolution. Black circles mark depth nodes with a resolution of less than 0.5. The circle diameter corresponds to the resolution, where circles with the largest diameter have a resolution of 0.95. For the bottom of the first layer 75 per cent of all depth nodes are well resolved. The depth nodes of this layer boundary are too numerous to be clearly arranged, and are therefore not displayed in the figure. (c) Plot of the ray coverage with rays modelling reflected and refracted waves. Different colours represent different phases.

that embedded small slivers of continental fragments, which may have broken off from earlier conjugate continental crust such as the Maurice Ewing Bank (Fig. 12a), still exist. However, plate-tectonic reconstructions show that before formation of the Agulhas Plateau, this region was occupied by the Maurice Ewing Basin (Fig. 12a), which makes it difficult to explain how continental fragments from the Maurice Ewing Bank could have been retained there. Therefore, the presence of large-scale continental fragments is rather unlikely.
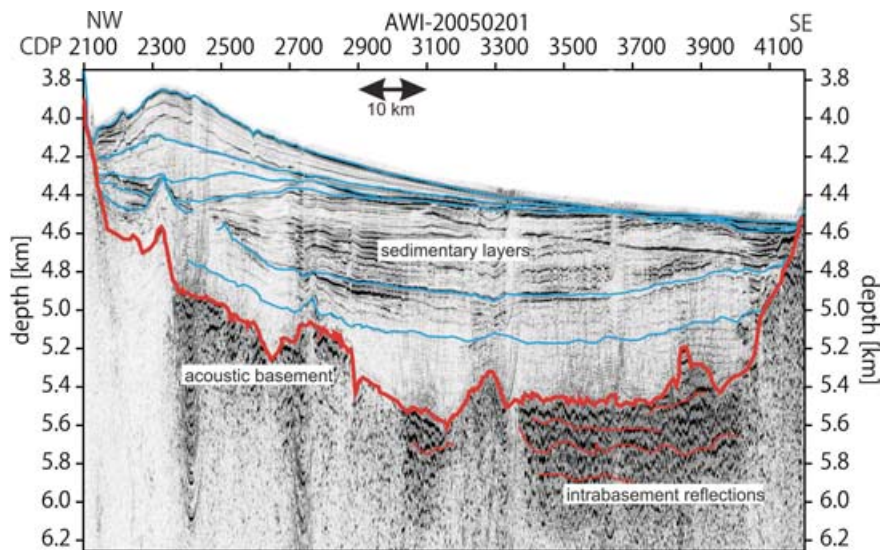
Figure 8. Depth-migrated seismic reflection section AWI-20050201 at the position of the Agulhas Passage showing thick sediments and intrabasement reflections interpreted as volcanic flows. Sediment layer boundaries marked with blue lines and some examples of intrabasement reflections are marked with thin red lines. The thick red line represents the top of the acoustic basement.
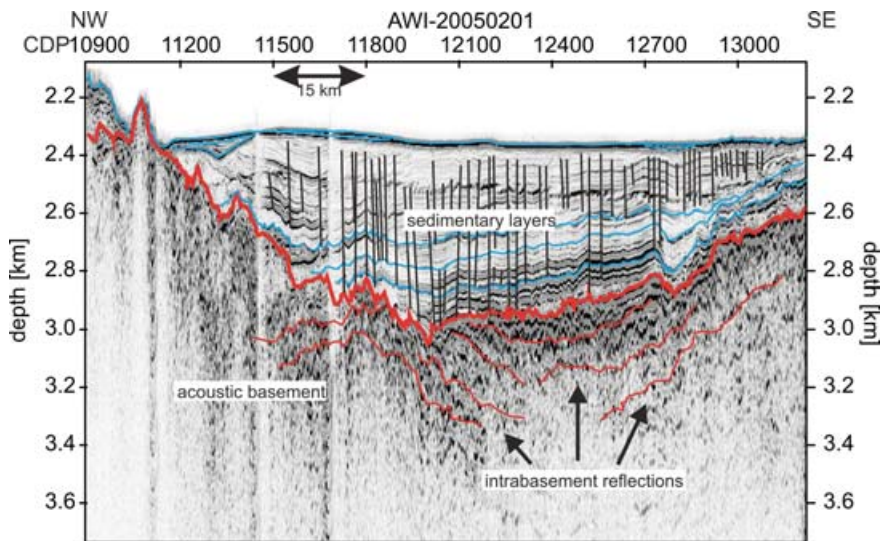

Figure 9. Depth-migrated seismic reflection section AWI-20050201 with intrabasement reflections (thin red lines) interpreted as volcanic flows.

Satellite-derived topography maps show two lineations (Fig. 2) striking in northeast–southwest direction in the region north of 38°S. Both of these lineations have coinciding lows in the ship-borne magnetic data at 370 and 440 km profile distance. Only the northern one (370 km) is observable in the velocity–depth model. Satellite magnetic data by CHAMP (Maus *et al.* 2007) (Fig. 2) show centres of negative anomalies aligned with the southern linear structure (440 km). The existence of these lineations suggests an extensional regime causing trench formation, which has plate-tectonic causes discussed in the next section.

6 THE AGULHAS PLATEAU LIP IN A PLATE-TECTONIC CONTEXT

Gohl & Uenzelmann-Neben (2001) estimate the time of plateau formation between 100 and 80 Ma, while a formation age of 120–96 Ma is inferred by Marks & Tikku (2001) using a revised plate-tectonic

reconstruction. We reconstructed the plate-kinematic situation in the region of the Agulhas Plateau to examine time and geometry of its formation. Rotation poles published by König & Jokat (2006) were used for the plate-tectonic reconstruction, where their rotation pole between South America and Africa for 130 Ma (centre: 50.00°N, 32.50°W; angle: 55.8°) was replaced by the rotation pole for 131.5 Ma (centre: 50.12°N, 32.79°W; angle: 55.2°) of Marks & Tikku (2001). The reconstruction shows that the Agulhas Plateau region was still occupied by the Maurice Ewing Basin (Fig. 12a) at 120 Ma, and therefore a formation as early as proposed by Marks & Tikku (2001) is unlikely. We place the time of the beginning of the Agulhas Plateau formation at about 100 ± 5 Ma (Figs 12b and c). At this time the plate-tectonic reconstructions show Maud Rise (MR) still attached to Agulhas Plateau (Fig. 12c). Northeast Georgia Rise (NEGR) and Agulhas Plateau (AP) overlap at 100 Ma (Fig. 12c). This overlap can be explained with the onset of LIP formation at that time, which did not have the same extent as today's
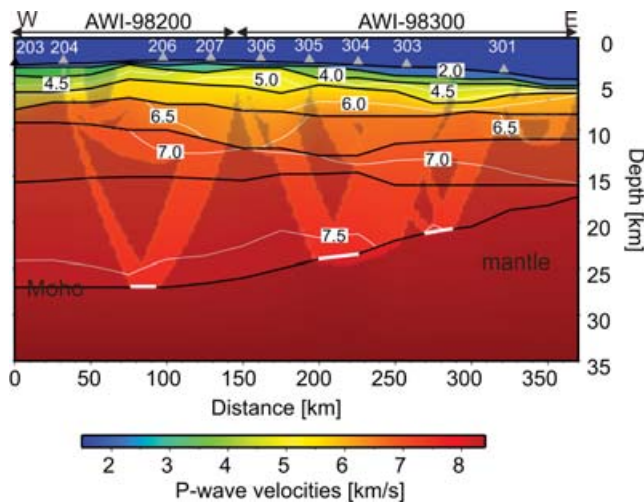
Figure 10. *P*-wave velocity–depth model of profiles AWI-98200 and AWI-98300 redrawn after Uenzelmann-Neben *et al.* (1999) and Gohl & Uenzelmann-Neben (2001).

fragments. Further rotation shows that at about 94 Ma (Fig. 12d) AP, MR and NEGR possibly had similar dimensions as today. The identification of extrusion centres in different depths in seismic reflection data suggests a crustal growth in at least two episodes (Gohl & Uenzelmann-Neben 2001). The first episode was probably at the beginning of the 6 Myr formation interval and caused the main crustal growth, while the second phase was initiated later possibly due to the fragmentation of the LIP. Extensional conditions during the fragmentation could be an explanation for the trench-like lineations observed on the Agulhas Plateau. On the central–southern plateau, any additional phases of excess volcanism may have masked evidence for extension in that region. Time estimates in the Cretaceous magnetic quiet time using plate-tectonic reconstruction are difficult and inexact. Lacking precise information from drilling on the Agulhas Plateau these reconstructions are a reasonable estimate to get an idea on possible formation ages and geometries.

It is not clear whether the magmatism of the Agulhas Plateau is linked to that of the Mozambique Ridge as discussed by Gohl

& Uenzelmann-Neben (2001). Plate-tectonic reconstructions (e.g. König & Jokat 2006) suggest that their crustal growth occurred most likely at different times and places. Marks & Tikku (2001) suspect that the gravity and topography high from the southwestern Mozambique Ridge to southern Agulhas Plateau might be the path of the Bouvet triple junction. If this is correct, a different formation time of Agulhas Plateau and Mozambique Ridge can be inferred. The Bouvet triple junction might have influenced the evolution of the Mozambique Ridge, moved southwestwards forming the topographic high east of the Agulhas Plateau and continued its motion, thus having an impact on the formation of Agulhas Plateau, Northeast Georgia Rise and Maud Rise. Therefore, the AP-NEGR-MR LIP may be an oceanic plateau that also formed at a triple junction such as the Shatsky Rise in the northwestern Pacific (Sager *et al.* 1999). The Bouvet hotspot, which was located at the northern part of the Agulhas Plateau 100 Ma ago according to Hartnady & le Roex (1985), may have contributed to the formation of the Agulhas Plateau in two ways. The distinct difference of the topography and basement structures between the northern and southern Agulhas Plateau was already recognized by Allen & Tucholke (1981) and suggests a non-uniform evolution of these parts. While the northern plateau is probably directly connected to the activity of the Bouvet hotspot, the southern plateau may have experienced a different history. Goergen *et al.* (2001) recognized interactions between the Bouvet and Marion hotspots with the Southwest Indian Ridge concluding that in the vicinity of spreading centres hotspot magmatism is enforced. Therefore, we suggest that the southern AP-MR-NEGR LIP formed as a result of excessive magmatism caused by the interaction between the Bouvet hotspot and the triple junction.

Today, wide regions in southern Africa and southwest of the African continent are characterized by anomalously elevated topography and shallow bathymetry, respectively. Together, these regions are called the African Superswell (Fig. 2) (Nyblade & Robinson 1994). Nyblade & Robinson (1994) suggested lithospheric heating as a possible cause. Plume events which date back to the Mesozoic are argued to be responsible for the anomalous elevation of the southern African plateau (Nyblade & Sleep 2003). Global seismic tomography studies identified a large scale low-velocity anomaly in the lower mantle beneath southern and southwestern Africa (Su *et al.* 1994), which is interpreted as the velocity expression of the African
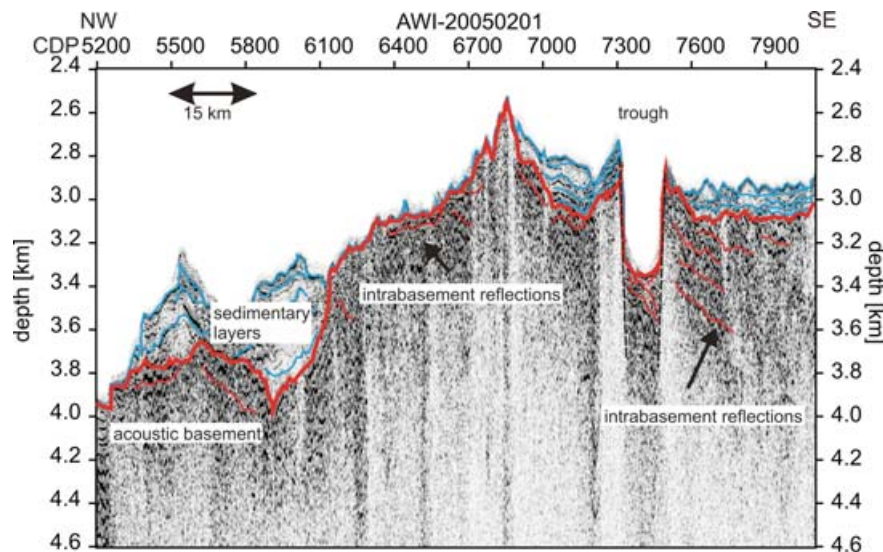

Figure 11. Depth-migrated seismic reflection section AWI-20050201 with graben-like structure in the northern Agulhas Plateau.
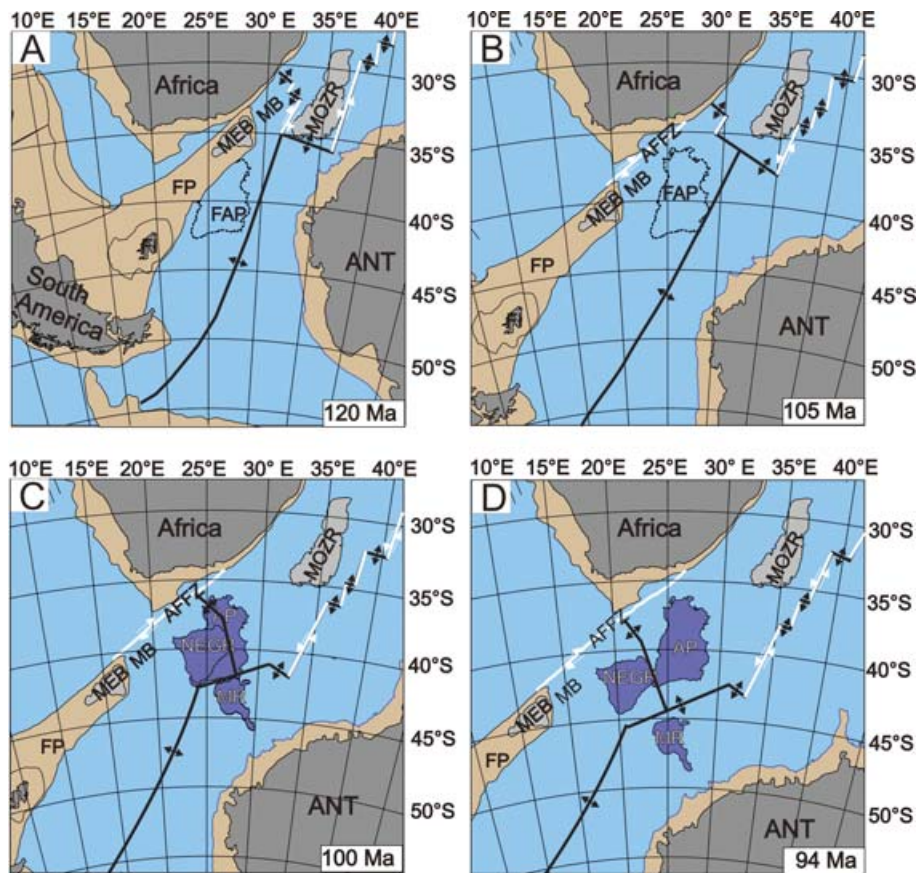
Figure 12. Plate-tectonic reconstructions using rotation poles published by König & Jokat (2006). The rotation was performed with respect to Africa. In figures (a–d) we use the present-day coordinate system for orientation. Thick lines sketch the estimated location of the palaeo-spreading system (black: spreading axis, white: transform fault). Abbreviations are AFFZ, Agulhas-Falkland Fracture Zone; ANT, Antarctica; AP, Agulhas Plateau; FAP, future position of Agulhas Plateau; FI, Falkland Islands; FP, Falkland Plateau; MB, Maurice Ewing Basin; MEB, Maurice Ewing Bank; MOZR, Mozambique Ridge; MR, Maud Rise and NEGR, Northeast Georgia Rise. (a) 120 Ma: Agulhas Plateau region was still occupied by Falkland Plateau with Maurice Ewing Bank leaving no space for the evolution of the Agulhas Plateau at this time. (b) 105 Ma: The Agulhas Plateau region was cleared. This is the first possibility for the formation of the AP. (c) 100 Ma: The reconstructions of Agulhas Plateau, Northeast Georgia Rise, and Maud Rise (but with the recent boundaries) show an overlap between Agulhas Plateau and Northeast Georgia Rise, which is due to different dimensions of these structures at 100 Ma. (d) 94 Ma: The formation of the whole LIP (AP, NEGR, MR) is complete. The Bouvet triple junction is located at the SW tip of the Agulhas Plateau (Marks & Tikku 2001), and subsequent spreading causes separation of the three fragments of the AP-NEGR-MR LIP.

Superplume (Ni & Helmberger 2003; Simmons *et al.* 2007). Class & le Roex (2006) state that the African Superswell has been a long-lived feature since 130–80 Ma. Burke & Torsvik (2004) suggest that low-velocity regions such as beneath the African Superswell have not changed their position with respect to the spin-axis of the Earth for the last 200 Ma. The low-velocity mantle anomaly beneath the African superswell (Lithgow-Bertelloni & Silver 1998; Ni & Helmberger 2003; Burke & Torsvik 2004) is interpreted to be caused by large-scale upwelling, which in turn can be considered as a plate driving force. It is reasonable to attribute the processes of continental breakup, triple junction activity, LIP formation and Bouvet hotspot activity to the mechanism of large-scale, enduring and distributed mantle upwelling of varying intensity and at different times.

7 CONSEQUENCES OF CRUSTAL GENERATION

7.1 Crustal volume of the Agulhas Plateau

The thickness of normal oceanic crust, that is, away from anomalous regions such as hotspot tracks, ranges between 5.0 and 8.5 km

(White *et al.* 1992). Regions of normal oceanic crust in the vicinity of the Agulhas Plateau have a thickness of about 6 km (Uenzelmann-Neben & Gohl 2004). The plateau's maximum crustal thickness of 24 km lies in the range of those of other comparable oceanic plateaus (20–40 km) (Coffin & Eldholm 1994). We calculated the excess crustal volume which is the additional volume compared to a 6-km-thick layer of normal oceanic crust, using thickness information from our seismic velocity–depth models (Figs 6a and 10) and seismic reflection records. The calculated excess crustal volume provides an important measure to quantify the amount of magmatic material involved in a LIP formation. The crustal thickness and volume calculations of the following paragraph are summarized in Table 3.

A bathymetry map (Fig. 1) is used to distinguish two zones of the AP which differ in their crustal thickness: zone a within the closed 3000 m depth contour and zone b between the 4000 and 3000 m depth contours (Fig. 13a). We calculated an area of 8.9×10^4 km^2 for zone a, 1.4×10^5 km^2 for zone b and 2.3×10^5 km^2 for the entire plateau (zone a + zone b). Crustal thicknesses in zone a are 24 km (at 125 km profile distance), 23 km (at 175 km) and 21 km (at 225 km) on profiles AWI-98200 and AWI-98300. On profile AWI-20050200,

Table 3. Steps for calculating the excess volume of the Agulhas Plateau with figures for the centre of the plateau within the 3000 m depth isoline (Fig. 13, zone *a*) and the area between the 3000 and 4000 m isolines (Fig. 13, zone *b*).

	Zone *a*	Zone *b*	Entire plateau
Area (10^5 km^2)	0.9	1.4	2.3
Av. crustal thickness (km)	16	21	18
Av. crustal volume (10^6 km^3)	1.9	2.2	4.1
Volume of normal oceanic crust, 6 km thickness (10^6 km^3)	0.5	0.8	1.3
Excess volume (10^6 km^3)	1.3	1.4	2.7
Extruded volume (10^6 km^3)	0.2	0.3	0.4
Intruded/LCB volume (10^6 km^3)	1.2	1.1	2.3

Note: Av., average; LCB, lower crustal body.

crustal thicknesses are 18 km (at 400 km), 19 km (at 500 km) and 20 km (at 600) in zone *a*. This leads to an average thickness for zone *a* of 21 km and a volume of 1.9×10^6 km^3. The crustal thickness of zone *b* is determined on profiles AWI-98200 and AWI-98300 to be 17 km (at 300 km profile length) and 24 km (at 50 km) thick. The latter value is derived from a poorly constrained part of the velocity model of profile AWI-98200 (Uenzelmann-Neben *et al.* 1999; Gohl & Uenzelmann-Neben 2001) and therefore not used here. Profile AWI-20050200 shows an average thickness of 15 km (at 300 km) for zone B. These results lead to an average crustal thickness of 16 km for zone B, which corresponds to a crustal volume of 2.2×10^6 km^3. The sum of both volumes is 4.1×10^6 km^3, which is between a maximum volume of 4.7×10^6 km^3 and a minimum

of 3.6×10^6 km^3 using 21 and 16 km as extreme values for the crustal thickness. Eldholm & Coffin (2000) summarize volumes of LIPs ranging from 0.7×10^6 km^3 for the Central Atlantic Magmatic province to 44.4×10^6 km^3 for the Ontong Java Plateau. Most LIP volumes are in the range of 2×10^6–1×10^7 km^3 (Eldholm & Coffin 2000), with the Agulhas Plateau having a comparable volume to that of the Caribbean LIP. Subtracting the volume of a 6-km-thick layer of oceanic crust in the area of the plateau leads to an excess magmatic volume of the plateau of 2.7×10^6 km^3.

We distinguished between an intruded/lower crustal body and an extruded component of the excess volume (Figs 13b and c). The extruded material is calculated using the average thickness of the layer of volcanic flows identified in the seismic reflection records (e.g. Fig. 9). Its thickness is estimated using velocity–depth models of profiles AWI-20050200, AWI-98200 and AWI-98300 (Figs 6 and 10) where the thickness of the layer with average velocities of between 3 and 5 km s^{-1} is sampled every 50 km. The average thickness is 1.8 km. This leads to an estimation of the extruded volume to be 0.4×10^6 km^3. The remaining excess volume of 2.3×10^6 km^3 intruded into oceanic crust and makes up the lower crustal body. Fig. 13 sketches the schematic structure of the Agulhas Plateau with its extrusive cover, intruded middle part (consisting of intruded middle and intruded lower crust) and its lower crustal body.

7.2 Thermal subsidence of the Agulhas Plateau

Discrimination between a marine or subaerial formation of the Agulhas Plateau is important to understand the influence of the excessive magmatism on the environment at the time of formation. Therefore,
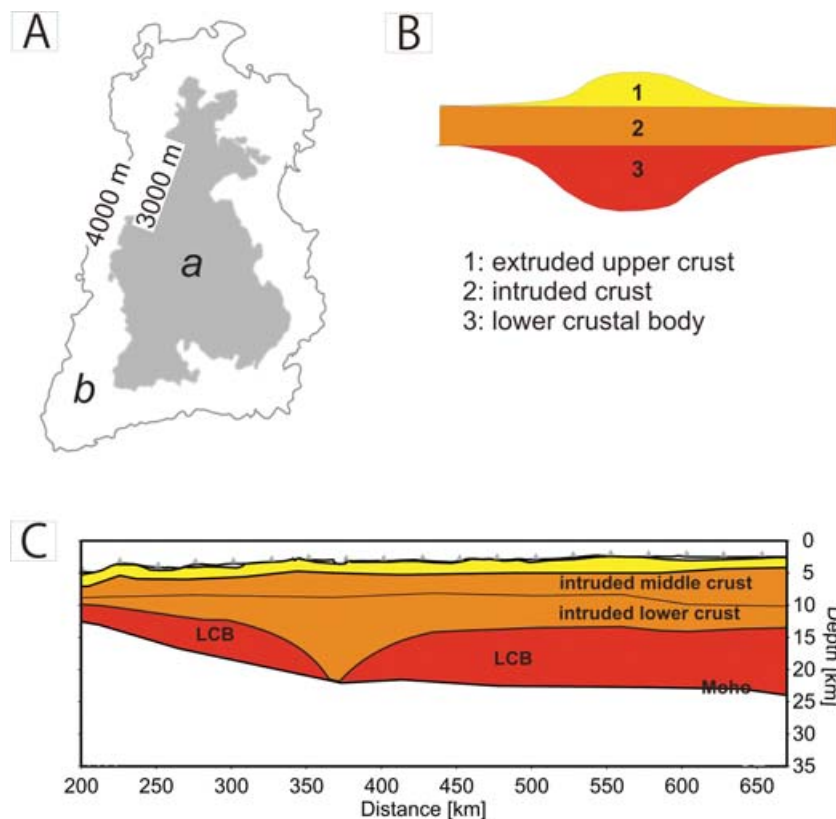

1: extruded upper crust
2: intruded crust
3: lower crustal body

Figure 13. (a) Subdivision of the Agulhas Plateau in zone *a* with average crustal thickness of 21 km and zone *b* with average thickness of 16 km. (b) General structure of an oceanic plateau LIP (Eldholm & Coffin 2000) consisting of an extrusive cover (yellow), an intruded middle part (orange) and lower crustal body (red). (c) Crustal structure of the Agulhas Plateau along profile AWI-20050200 showing the typical structure of a LIP.

Table 4. Calculation of the thermal subsidence of the Agulhas Plateau between 100 and 80 Ma using the approximation formula after Parsons & McKenzie (1978) for typical water depth values of 4000 and 3000 m.

Age (Ma)	Depth (m)	Paleo-depth (m)
100	4000	750
100	3000	−250
95	3000	−200
90	3000	−140
85	3000	−70
80	3000	−10

we calculated the influence of subsidence, which led to the present depth of the Agulhas Plateau between 2000 and 4000 m below sea level (Fig. 1). In order to estimate the palaeo-depth of the Agulhas Plateau between 100 and 80 Ma, the thermal subsidence of the Agulhas Plateau was calculated using the equation of Parsons & McKenzie (1978) for the 3000 and 4000 m depth isolines (Table 4). We calculated paleo-depths of at least 250 m above sea level for the area within the present 3000 m isobath of the Agulhas Plateau (Table 4). If the central part of the plateau (within the 3000 m depth isoline) already existed at 100 Ma, it was possibly subaerial, and stayed above the water surface for a maximum of 20 Myr (Table 4). We did not include the additional subsidence due to loading, because our data does not provide evidence if the basalt flows on the Agulhas Plateau were erupted on already overthickened crust or occurred at the same time as crustal thickening. Therefore, the calculated subsidence is a minimum value, leading to the consequence that larger areas of the Agulhas Plateau could have been subaerial. Changes in sea level were not included in the calculations but are small enough (e.g. Skelton 2003) not to change the conclusion of a partly subaerial early Agulhas Plateau.

7.3 Estimation and implication of gas emissions during LIP formation

Estimations of gas emission volumes and rates of Large Igneous Provinces are sparsely published (e.g. Caldeira & Rampino 1990; Self *et al.* 2005) although the impact of LIP formation on climate, environment and their possible correlation to mass extinctions is often discussed (e.g. Coffin & Eldholm 1994; Wignall 2001; Kerr 2005; Wignall 2005). So far, gas emission volumes have only been estimated for continental flood basalt type LIPs but not for oceanic plateaus (e.g. Caldeira & Rampino 1990; Self *et al.* 2005). Such calculations are more difficult for oceanic plateaus due to their formation in a marine environment. Interactions with surrounding water such as solution or other chemical reactions are difficult to take into account. We have shown that a large part of the Agulhas Plateau possibly formed subaerially and we therefore use information from gas emissions of flood basalt provinces as a guiding example to estimate the amount of released gases during the Agulhas Plateau formation.

Caldeira & Rampino (1990) estimated 6×10^{10} moles carbon dioxide per cubic kilometres magma for the Deccan traps. Using our calculated volume of 0.4×10^6 km^3 of extrusives, we can derive 2.5×10^{16} moles carbon dioxide, which corresponds to a mass of 1.1×10^{12} t. Self *et al.* (2005) state a value of 13×10^6 t carbon dioxide emission per cubic kilometres of lava, which results in a total amount of 5.4×10^{12} t of released carbon dioxide during Agulhas Plateau formation. In comparison, the Deccan traps emitted between 6×10^{16} and 2×10^{17} mol (2.6–8.8 $\times 10^{12}$ t) carbon dioxide (Caldeira & Rampino 1990). Our value for the Agulhas Plateau

carbon dioxide emission is a rough estimate due to the assumptions mentioned before.

Self *et al.* (2005) estimated a release of 5–10 $\times 10^6$ t sulphur dioxide per cubic kilometres of magmatic material during flood basalt eruptions. Again, we use the information of a subaerial early Agulhas Plateau as a qualification to use Self *et al.*'s (2005) value for an estimation of sulphur dioxide amounts released during the plateau formation. Using these assumptions we calculate a release of 2.0–4.0 $\times 10^{12}$ t sulphur dioxide. Drilling and petrological analysis of the core material measuring pre- and post-eruption sulphur dioxide contents (Self *et al.* 2005) could lead to a better estimate, but this information does not exist so far.

Carbon dioxide emission during the larger AP-NEGR-MR LIP formation was more than double that produced during the Agulhas Plateau development. However, since this amount was released in a 6 Myr long time interval (but most likely in shorter episodes during this interval), which would correspond to 0.4–2.0 $\times 10^6$ t yr^{-1} on average, it is negligible when compared to the anthropogenic carbon dioxide emission of ~10^{10} t yr^{-1} (e.g. Wignall 2001; Saunders 2005; Wignall 2005). A comparison with the carbon dioxide release of the Deccan traps of 2.6–8.8 $\times 10^{12}$ t (Caldeira & Rampino 1990) demonstrates that the emission of the AP-NEGR-MR LIP (~2.4 to 11.7 $\times 10^{12}$ t) is of the same order of magnitude. Caldeira & Rampino (1990) calculated that carbon dioxide released by the Deccan trap basalts caused a maximum temperature increase of 1 °C over a period of a few hundred thousand years. Consequently, the formation of the AP-NEGR-MR LIP could have caused a similar effect but possibly over a longer time scale. However, more reliable estimates for any climatic impact of this LIP complex can only be performed by deriving the timing and intensity of the volcanic eruption phases and rates from analyses of drilled rock samples.

8 CONCLUSIONS

The Agulhas Plateau consists of 20-km-thick crust. Intrabasement reflections identified in the seismic reflection records were interpreted as volcanic flows which make up the upper part of the crust with seismic velocities of 4.1 km s^{-1} on average. In the middle crust average *P*-wave velocities of 6.0 km s^{-1} are modelled. The lower crust has an average velocity of 7.2 km s^{-1}, where the lower 10 km of the crust show high velocities between 7.0 and 7.6 km s^{-1}. This velocity–depth structure leads to the conclusion that the Agulhas Plateau consists of overthickened oceanic crust. A small part of the lower crust shows lower velocities than the surrounding areas. Due to these velocities small continental fragments are possible there, but unlikely due to plate-tectonic reasons. The Agulhas Plateau shows a similar velocity–depth structure as oceanic LIPs and consists of the same structural units: an extrusive cover, an intruded middle part and a lower crustal body. This implies that the Agulhas Plateau is a Large Igneous Province of oceanic affinity.

A plate-tectonic reconstruction was used to demonstrate a likely joint formation of Agulhas Plateau, Northeast Georgia Rise and Maud Rise with the Bouvet triple junction in the centre of the LIP. It is possible that an interaction between the Bouvet triple junction and the Bouvet hotspot caused the formation of this LIP, which was fragmented due to spreading processes. We estimated the beginning of the LIP generation at 100 ± 5 Ma and the end at 94 ± 5 Ma. Graben-like structures on the northern Agulhas Plateau were interpreted as remnant structures caused by extensional forces which acted during the fragmentation of the AP-NEGR-MR LIP. Any

extensional features on the central–southern plateau were overprinted by later phases of magmatism.

We used two perpendicular velocity–depth models of the Agulhas Plateau to estimate its total volume to be 4.1×10^6 km^3 and the excess crustal volume to be 2.7×10^6 km^3. The extruded part of the excess volume is 0.4×10^6 km^3 and the volume of the intruded/LCB materials is 2.3×10^6 km^3. Thermal subsidence calculations suggest that major parts of the Agulhas Plateau have probably formed subaerially, causing a direct emission of released volcanic gases into the atmosphere. Knowing the volume of the extrusive component, we estimate carbon dioxide (1.1–5.4×10^{12} t) and sulphur dioxide (2.0–4.0×10^{12} t) emission during Agulhas Plateau formation. Although an interpretation is difficult because emission rates are more important than the total amount of emitted gases, these values provide an interesting input to the discussion of climate impact of LIPs as estimations of gas emissions of individual LIPs have been put forward rarely in the past.

REFERENCES

Allen, R.B. & Tucholke, B.E., 1981. Petrology and implications of continental rocks from the Agulhas Plateau, southwest Indian Ocean, *Geology, 9,* 463–468.

Angevine, C.L. & Turcotte, D.L., 1983. Correlation of geoid and depth anomalies over the Agulhas Plateau, *Tectonophysics, 100,* 43–52.

Barrett, D.M., 1977. The Agulhas Plateau off southern Africa: a geophysical study, *Geol. Soc. Am. Bull., 88,* 749–763.

Burke, K. & Torsvik, T.H., 2004. Derivation of large igneous provinces of the past 200 million years from long-term heterogeneities in the deep mantle, *Earth planet. Sci. Lett., 227,* 531–538.

Caldeira, K. & Rampino, M.R., 1990. Carbon dioxide emissions from Deccan volcanism and K/T boundary greenhouse effect, *Geophys. Res. Lett., 17,* 1299–1302.

Charvis, P., Recq, M., Operto, S. & Bretort, D., 1995. Deep structure of the northern Kerguelen Plateau and hotspot-related activity, *Geophys. J. Int., 122,* 899–924.

Class, C. & le Roex, A.P., 2006. Continental material in the shallow oceanic mantle—how does it get there? *Geology, 34,* 129–132.

Coffin, M.F. *et al.*, 2006. Large igneous provinces and scientific ocean drilling, *Oceanography, 19,* 150–160.

Coffin, M.F. & Eldholm, O., 1994. Large igneous provinces: crustal structure, dimensions, and external consequences, *Rev. Geophys., 32,* 1–36.

de Wit, M. & Horsfield, B., 2006. Inkaba yeAfrica project surveys sector of earth from core to space, *EOS Trans. AGU, 87,* 113–117.

Eldholm, O. & Coffin, M.F., 2000. Large igneous provinces and plate tectonics, *Geophys. Mon., 121,* 309–326.

Eldholm, O. & Grue, K., 1994. North atlantic volcanic margins: dimensions and production rates, *J. geophys. Res., 99,* 2955–2968.

Gladczenko, T.P., Coffin, M.F. & Eldholm, O., 1997. Crustal structure of the Ontong Java Plateau: modeling new gravity and existing seismic data, *J. geophys. Res., 102,* 22 711–22 729.

Goergen, J.E., Lin, J. & Dick, H.J.B., 2001. Evidence from gravity anomalies for interactions of the Marion and Bouvet hotsports with the Southwest Indian Ridge: effects of transform offsets, *Earth planet. Sci. Lett., 187,* 283–300.

Gohl, K. & Uenzelmann-Neben, G., 2001. The crustal role of the Agulhas Plateau, southwest Indian Ocean: evidence from seismic profiling, *Geophys. J. Int., 144,* 632–646.

Hartnady, C.J.H. & le Roex, A.P., 1985. Southern Ocean hotspot tracks and the Cenozoic absolute motion of the African, Antarctic, and South American plates, *Earth planet. Sci. Lett., 75,* 245–257.

Kerr, A.C., 2005. Oceanic LIPs: the kiss of death, *Elements, 3,* 289–292.

König, M. & Jokat, W., 2006. The Mesozoic breakup of the Weddell Sea, *J. geophys. Res., 111,* doi:10.1029/2005JB004035.

Kristoffersen, Y. & LaBrecque, J., 1991. On the tectonic history and origin of the Northeast Georgia Rise, *Proc. ODP, Scient. Res., 114,* 23–38.

Lithgow-Bertelloni, C. & Silver, P.G., 1998. Dynamic topography, late driving forces and the African superswell, *Nature, 395,* 269–271.

Marks, K.M. & Tikku, A.A., 2001. Cretaceous reconstructions of East Antarctica, Africa and Madagascar, *Earth planet. Sci. Lett., 186,* 479–495.

Martin, A.K., 1987. Plate reorganisations around Southern Africa, hot spots and extinctions, *Tectonophysics, 142,* 309–316.

Maus, S., Lühr, H., Rother, M., Hemant, K., Balasis, G., Ritter, P. & Stolle, C., 2007. Fifth-generation lithospheric magnetic field model from CHAMP satellite measurements, *Geochem. Geophys. Geosyst., 8,* doi:10.1029/2006GC001521.

Ni, S. & Helmberger, D., 2003. Seismological constraints on the South African superplume; could be oldest distinct structure on earth, *Earth planet. Sci. Lett., 206,* 119–131.

Nyblade, A.A. & Robinson, W.S., 1994. The African superswell, *Geophys. Res. Lett., 21,* 765–768.

Nyblade, A.A. & Sleep, N.H., 2003. Long lasting epeirogenic uplift from mantle plumes and the origin of the Southern African Plateau, *Geochem. Geophys. Geosyst., 4,* doi:10.1029/2003GC000573.

Operto, S. & Charvis, P., 1996. Deep structure of the southern Kerguelen Plateau (southern Indian Ocean) from ocean bottom seismometer wide-angle seismic data, *J. geophys. Res., 101,* 25 077–25 103.

Parsiegla, N., Gohl, K. & Uenzelmann-Neben, G., 2007. Deep crustal structure of the sheared South African continental margin: first results of the Agulhas-Karoo Geoscience Transect, *S. Afric. J. Geol., 110,* 393–406, doi:10.2113/gssajg.110.2/3.393.

Parsons, B. & McKenzie, D., 1978. Mantle convection and the thermal structure of plates, *J. geophys. Res., 83,* 4485–4496.

Sager, W.W., Kim, J., Klaus, A., Nakanishi, M. & Khankishieva, L.M., 1999. Bathymetry of Shatsky Rise, northwest Pacific Ocean: Implications for oceanic plateau formation at a triple junction, *J. geophys. Res., 104,* 7557–7576.

Saunders, A.D., 2005. Large igneous provinces: origin and environmental consequences, *Elements, 1,* 259–263.

Scrutton, R.A., 1973. Structure and evolution of the sea floor south of South Africa, *Earth planet. Sci. Lett., 19,* 250–256.

Self, S., Thordarson, T. & Widdowson, M., 2005. Gas fluxes from flood basalt eruptions, *Elements, 1,* 283–287.

Simmons, N.A., Forte, A.M. & Grand, S.P., 2007. Thermochemical structure and dynamics of the African superplume, *Geophys. Res. Lett., 34,* doi:10.1029/2006GL028009.

Skelton, P., 2003. Fluctuating sea-level, in *The Cretaceous World,* pp. 67–83, ed. Skelton, P. Cambridge University Press, Cambridge.

Smith, W.H.F. & Sandwell, D.T., 1997. Global seafloor topography from satellite altimetry and ship depth soundings, *Science, 277,* 1957–1962.

Su, W.J., Woodward, R.L. & Dziemonski, A.M., 1994. Degree 12 model of shear velocity heterogeneity in the mantle, *J. geophys. Res., 99,* 6945–6980.

Tucholke, B.E., Houtz, R.E. & Barrett, D.M., 1981. Continental crust beneath the Agulhas Plateau, southwest Indian Ocean, *J. geophys. Res.,* **86,** 3791–3806.

Uenzelmann-Neben, G. & Gohl, K., 2004. The Agulhas Ridge, South Atlantic: the peculiar structure of a fracture zone, *Mar. geophys. Res.,* **25,** 305–319.

Uenzelmann-Neben, G., Gohl, K., Ehrhardt, A. & Seargent, M., 1999. Agulhas Plateau, SW Indian Ocean: new evidence for excessive volcanism, *Geophys. Res. Lett.,* **26,** 1941–1944.

Uenzelmann-Neben, G., 2005. Southeastern Atlantic and southwestern Indian Ocean: reconstruction of sedimentary and tectonic development since the Cretaceous, AISTEK I: Agulhas Transect, *Berichte zur Polar- und Meeresforschung* **515,** 1–73.

Voss, M. & Jokat, W., 2007. Continent-ocean transition and voluminous magmatic underplating derived from P-wave velocity modelling of the East Greenland continental margin, *Geophys. J. Int.,* **170,** 580–604.

Wessel, P. & Smith, W.H.F., 1998. New, improved version of generic mapping tools released, *EOS Trans. AGU,* **79,** 579.

White, R.S., McKenzie, D. & O'Nions, R.K., 1992. Oceanic crustal thickness from seismic measurements and rare earth element inversions, *J. geophys. Res.,* **97,** 19 683–19 715.

Wignall, P.B., 2001. Large igneous provinces and mass extinctions, *Earth-Sci. Rev.,* **53,** 1–33.

Wignall, P.B., 2005. The link between large igneous province eruptions and mass extinctions, *Elements,* **1,** 293–297.

Yilmaz, Ö., 2001. Seismic data analysis: processing, inversion, and interpretation of seismic data, in *Investigations in Geophysics,* pp. 1000, ed. Doherty, S.M. Society of Exploration Geophysics, Tulsa.

Zelt, C.A. & Smith, R.B., 1992. Seismic traveltime inversion for 2-D crustal velocity structure. *Geophys. J. Int.,* **108,** 16–34.

Zelt, C.A. & White, D.J., 1995. Crustal structure and tectonics of the southeastern Canadian Cordillera, *J. geophys. Res.,* **100,** 24 255–24 273.